Journal of Solid State Chemistry 181 (2008) 2237–2242

Contents lists available at ScienceDirect

Journal of Solid State Chemistry

journal homepage: www.elsevier.com/locate/jssc

Hydrothermal assembly and luminescence property of lanthanide-containing Anderson polyoxometalates

Ying Liu, Shu-Xia Liu *, Rui-Ge Cao, Hong-Mei Ji, Shi-Wei Zhang, Yuan-Hang Ren

Key Laboratory of Polyoxometalates Science of Ministry of Education, College of Chemistry, Northeast Normal University, Changchun City, JiLin 130024, PR China

ARTICLE INFO

Article history:
Received 20 December 2007
Received in revised form
5 May 2008
Accepted 7 May 2008
Available online 21 May 2008

Keywords:
Polyoxometalate
Anderson-type polyoxoanion
Hydrothermal synthesis
Fluorescence

ABSTRACT

Two compounds, $\{[Sm(H_2O)_5]_2(TeMo_6O_{24})\}\cdot 6H_2O$ (**1**) and $\{[Eu(H_2O)_7]_2\ (TeMo_6O_{24})\}\cdot 5H_2O$ (**2**) have been synthesized by hydrothermal reactions and characterized by elemental analyses, IR spectra, thermal stability analyses, X-ray powder diffraction, and single-crystal X-ray diffraction. Compound **1** represents the first example of a 2D layer architecture constructed from Anderson-type polyoxoanions $[TeMo_6O_{24}]^{6-}$ and rare-earth ions Ln^{3+}. Compound **2** displays a 1D chain structure built up of alternating Anderson-type polyoxoanions $[TeMo_6O_{24}]^{6-}$ and rare-earth ions Eu^{3+} along the *c*-axis. Luminescence measurement of **2** exhibits typical red fluorescent emission of the Eu^{3+} ion at room temperature. Furthermore, the emission is intense enough to be observed macroscopically under UV irradiation (365 nm).

1. Introduction

Polyoxometalates (POMs) chemistry has been extensively investigated for many years due to the fascinating class of metal–oxygen cluster compounds possessing a unique structural variety and interesting properties, which are of use in different fields including catalysis, medicine, magnetism, and optics [1–5]. A current challenging task of the POMs chemistry focuses on employing various polyoxoanions as inorganic building blocks to exploit novel materials with special structures and cooperative properties. One branch of this area is the incorporation of the lanthanide ions Ln^{3+} in such POMs not only because of their interesting luminescent and magnetic properties, but also owing to their multiple coordination requirements and oxophilicity, which are suitable for linking up discrete polyoxoanion units into 1D, 2D, and even 3D frameworks [6–9].

As an important subclass of POMs, Anderson-type polyoxoanions exhibit planar structures and have abundant terminal oxygen atoms, which make them possess high reactivity and then readily coordinate to rare-earth metal centers. In 2002, Das and coworkers [10] reported a 1D chain compound constructed from $[Al(OH)_6Mo_6O_{18}]^{3-}$ polyoxoanion and the La^{3+} ion for the first time. Followed by this, Krebs and coworkers [11–13] reported a series of Lanthanide compounds based on $[TeMo_6O_{24}]^{6-}$ polyoxoanion, exhibiting 1D chain structures. In addition, Wang and coworkers [15–17] have also obtained several compounds built up of $[Cr(OH)_6Mo_6O_{18}]^{3-}$ or $[IMo_6O_{24}]^{5-}$ polyoxoanions and rare-earth ions or rare-earth coordination complexes in recent years. It is noteworthy that all of these compounds were synthesized by the conventional solution method. More recently, our group has successfully synthesized a series of 3D compounds holding rutile-like topology with $[TeMo_6O_{24}]^{6-}$ polyoxoanion and rare-earth cations under hydrothermal conditions [18], which indicates that the $[TeMo_6O_{24}]^{6-}$ polyoxoanion is also stable in hydrothermal conditions. As a part of our ongoing work, we have investigated the reaction of the $[TeMo_6O_{24}]^{6-}$ polyoxoanion and rare-earth ions by changing the reaction conditions in hydrothermal synthesis, such as starting materials, stoichiometry, pH value, filling volume and temperature, and obtained two compounds formulated as $\{[Sm(H_2O)_5]_2(TeMo_6O_{24})\}\cdot 6H_2O$ (**1**) and $\{[Eu(H_2O)_7]_2(TeMo_6O_{24})\}\cdot 5H_2O$ (**2**). Compound **1** represents the first example of a 2D layer architecture constructed from polyoxoanion $[TeMo_6O_{24}]^{6-}$ and rare-earth ions. Compound **2** displays a 1D chain structure constructed from alternating polyoxoanions $[TeMo_6O_{24}]^{6-}$ and rare-earth ions Eu^{3+} along the *c*-axis. From a number of parallel experiments, it was found that changes in reaction temperature led to different structures when other reaction parameters maintained unaltered, indicating that temperature played an important role in the formation of the resultants. Luminescence measurement reveals that **2** exhibits typical red fluorescent emission of the Eu^{3+} ion at room temperature. The brilliant red luminescence of samples is macroscopical under UV irradiation (365 nm), which indicates that the emission is intense.

* Corresponding author. Fax: +86 431 85099328.
E-mail address: liusx@nenu.edu.cn (S.-X. Liu).

0022-4596/$ - see front matter © 2008 Published by Elsevier Inc.
doi:10.1016/j.jssc.2008.05.023

2. Experimental

2.1. Materials

All chemicals were used as purchased without further purification. Elemental analyses (Sm, Eu, Te, and Mo) were performed on a PLASMA-SPEC(I) ICP atomic emission spectrometer. IR spectra were recorded in the range 400–4000 cm^{-1} on an Alpha Centaurt FT/IR spectrophotometer using KBr pellets. Powder X-ray diffraction measurements were performed on a Rigaku D/MAX-3 instrument with Cu-$K\alpha$ radiation in the angular range $2\theta = 3$–50° at 293 K. Thermal stability analyses were performed on a Perkin-Elmer TGA7 instrument in N_2 atmosphere with a heating rate of 10 °C/min. Luminescence measurement was carried out on a Hitachi F-4500 Fluorescence Spectrophotometer.

2.2. Syntheses of compounds **1** and **2**

2.2.1. $\{[Sm(H_2O)_5]_2(TeMo_6O_{24})\}\cdot 6H_2O$ (**1**)

A mixture of TeO_2 (0.11 g, 0.7 mmol), $Na_2MoO_4\cdot 2H_2O$ (1.01 g, 4.2 mmol), NaOH (0.06 g, 1.4 mmol), $SmCl_3\cdot 6H_2O$ (0.36 g, 1.0 mmol), H_2O_2 (30%, 0.5 mL), and H_2O (10 mL) was stirred in air for 30 min after the pH was adjusted to 2.7 with HCl (4 M). The resulting suspension was sealed in a 16 mL Teflon-lined stainless-steel autoclave, which was kept at 130 °C for 3 days, then cooled to room temperature at 6 °C/h. The colorless block crystals were filtered and washed with distilled water (83% yield based on Te). Anal. calcd. for $H_{32}TeSm_2Mo_6O_{40}$ (%): Sm, 17.93; Te, 7.61; Mo, 34.34. Found: Sm, 17.78; Te, 7.80; Mo, 34.52. IR (KBr pellet, cm^{-1}) for (**1**): 3417(br), 1613(m), 939(s), 893(m), 674(m), 610(s), 539(s), 445(s).

2.2.2. $\{[Eu(H_2O)_7]_2(TeMo_6O_{24})\}\cdot 5H_2O$ (**2**)

The preparation of **2** was similar to that of **1**, except that $EuCl_3\cdot 6H_2O$ (0.37 g, 1.0 mmol) was used in place of $SmCl_3\cdot 6H_2O$ (0.36 g, 1.0 mmol), and the temperature for 110 °C (81% yield based on Te). Anal. calcd. for $H_{38}TeEu_2Mo_6O$ (%): Eu, 17.53; Te, 7.36; Mo, 33.20. Found: Eu, 17.62; Te, 7.34; Mo, 33.12. IR (KBr pellet, cm^{-1}) for (**2**): 3409(br), 1622(m), 947(s), 908(m), 681(m), 610(s), 538(s), 445(s).

2.3. X-ray crystallography

Diffraction intensities for compound **1** were collected on a Rigaku R-AXIS RAPID IP diffractometer (a SMART CCD diffractometer for **2**) with Mo $K\alpha$ monochromatic radiation ($\lambda = 0.71073$ Å) at 293 K. The linear absorption coefficients, scattering factors for the atoms, and anomalous dispersion corrections were taken from International Tables for X-ray crystallography. The structures of **1** and **2** were solved by the direct method and refined by the full-matrix least-squares method on F^2 using the SHELXTL crystallographic software package [19]. All non-hydrogen atoms in **1** and **2** were refined anisotropically. The hydrogen atoms from parts of water molecules were located from the difference Fourier maps. For the compounds, the voids of the structures are occupied by some disordered lattice waters, which show many peaks of low electronic density in the difference Fourier maps. The numbers of lattice waters for the compounds are determined by thermogravimetric analyses. The crystal data and structure refinement results of compounds **1** and **2** are summarized in Table 1. Selected bond lengths and bond angles for compounds **1** and **2** are provided in Tables S1 and S2 in the supporting material, and the selected Ln–O bond lengths and bond angles, which are also significant for the lanthanide coordination or for the BVS calculations are presented in Table 2. Further details of the crystal structure investigations of **1** and **2** may be obtained from the Fachinformationszentrum Karlsruhe, D-76344 Eggenstein-Leopoldshafen, Germany (e-mail: Crysdata@fiz-karlstruhe.de) on quoting the deposited numbers CSD-418876, CSD-418877, respectively. The experimental and simulated X-ray powder diffraction patterns (XRPD) of both compounds are shown in Fig. S1. The diffraction peaks on both experimental and simulated patterns match well in position, indicating their phase purity.

Table 1
Crystal data and structure refinement parameters for **1** and **2**

	1	**2**
Empirical formula	$H_{20}TeSm_2Mo_6O_{36}$	$H_{24}TeEu_2Mo_6O_{43}$
M	1600.12	1719.37
Crystal system	Triclinic	Triclinic
Space group	P-1	P-1
θ range (deg)	3.39–27.49	2.25–28.45
a (Å)	8.9533(18)	9.5490(5)
b (Å)	9.3365(19)	10.2479(5)
c (Å)	10.458(2)	11.6300(10)
α (Å)	72.32(3)	97.9070(10)
β (Å)	77.02(3)	101.4740(10)
γ (Å)	70.40(3)	114.4290(10)
V (Å^3)	777.2(3)	984.18(11)
Z	1	1
F(000)	736	798
D_c (g cm^{-3})	3.418	2.901
Abs coeff (mm^{-1})	7.094	5.829
Total data collected	7674	5343
Unique data	3530	3818
R_{int}	0.0432	0.0252
GOF	1.139	1.163
R_1 [$I>2\sigma(I)$][a]	0.0379	0.0442
wR_2 (all data)[b]	0.0961	0.1208

[a] $R_1 = \Sigma\|F_o\|-|F_c\|/\Sigma|F_o|$.
[b] $wR_2 = [\Sigma w(F_o^2-F_c^2)^2/\Sigma w(F_o^2)^2]^{1/2}$.

Table 2
Ln–O bond lengths (Å) and bond angles (deg) of compounds **1** and **2**

1		**2**	
Sm(1)–O(24)	2.446(5)	Eu(1)–O(22)	2.440(6)
Sm(1)–O(10)♯2	2.424(5)	Eu(1)–O(13)	2.441(5)
Sm(1)–O(7)	2.432(5)	Eu(1)–O(16)	2.446(5)
Sm(1)–O(22)	2.435(5)	Eu(1)–O(21)	2.451(5)
Sm(1)–O(23)	2.446(6)	Eu(1)–O(14)	2.452(4)
Sm(1)–O(21)	2.463(5)	Eu(1)–O(18)	2.460(5)
Sm(1)–O(25)	2.495(6)	Eu(1)–O(17)	2.466(4)
Sm(1)–O(8)♯3	2.501(5)	Eu(1)–O(8)♯2	2.491(5)
Sm(1)–O(20)♯4	2.540(5)	Eu(1)–O(20)	2.515(5)
O(10)♯2–Sm(1)–O(7)	87.76(17)	O(22)–Eu(1)–O(13)	134.8(2)
O(10)♯2–Sm(1)–O(22)	137.40(18)	O(22)–Eu(1)–O(16)	80.5(2)
O(7)–Sm(1)–O(22)	73.25(17)	O(13)–Eu(1)–O(16)	71.86(18)
O(10)♯2–Sm(1)–O(23)	76.66(19)	O(22)–Eu(1)–O(21)	72.1(3)
O(7)–Sm(1)–O(23)	136.6(2)	O(13)–Eu(1)–O(21)	66.62(19)
O(22)–Sm(1)–O(23)	141.62(19)	O(16)–Eu(1)–O(21)	74.93(19)
O(10)♯2–Sm(1)–O(24)	138.08(17)	O(22)–Eu(1)–O(14)	83.7(2)
O(7)–Sm(1)–O(24)	79.56(17)	O(21)–Eu(1)–O(14)	135.57(17)
O(24)–Sm(1)–O(21)	139.52(17)	O(22)–Eu(1)–O(18)	135.1(2)
O(23)–Sm(1)–O(25)	69.5(2)	O(14)–Eu(1)–O(18)	87.65(16)
O(24)–Sm(1)–O(25)	69.26(19)	O(22)–Eu(1)–O(17)	142.8(2)
O(21)–Sm(1)–O(25)	134.9(2)	O(13)–Eu(1)–O(17)	68.69(16)

Symmetry codes for **1**: ♯1: $-x$, $-y+1$, $-z+2$; ♯2: $x+1$, $y-1$, z; ♯3: $x+1$, y, z; ♯4: $-x+1$, $-y$, $-z+2$; ♯5: $x-1$, y, z; ♯6: $x-1$, $y+1$, z; symmetry codes for **2**: ♯1: $-x+1$, $-y+2$, $-z+1$; ♯2: $-x+1$, $-y+1$, $-z+1$.

3. Results and discussion

3.1. Syntheses

The compounds have been successfully synthesized by choosing TeO_2 and $Na_2MoO_4 \cdot 2H_2O$ as starting materials. In such a synthesis system, the addition of NaOH and H_2O_2 is essential. NaOH promotes the dissolution of tellurium dioxide to form the soluble tellurite, and H_2O_2 as the oxidant can oxidize Te^{IV}–Te^{VI} so as to form the polyoxoanion $[TeMo_6O_{24}]^{6-}$. Compounds **1** and **2** were both obtained based on Anderson-type anion $[TeMo_6O_{24}]^{6-}$ under mild hydrothermal conditions. The formation process and reaction equations can be described as

$$TeO_2 + 2OH^- = TeO_3^{2-} + H_2O \quad (1)$$

$$TeO_3^{2-} + H_2O_2 + H_2O = TeO_6^{6-} + 4H^+ \quad (2)$$

$$6[MoO_4]^{2-} + TeO_6^{6-} + 12H^+ = [TeMo_6O_{24}]^{6-} + 6H_2O \quad (3)$$

$$2Ln^{3+} + (2m+n)\,H_2O + [TeMo_6O_{24}]^{6-} = \{[Ln(H_2O)_m]_2(TeMo_6O_{24})\} \cdot nH_2O \quad (4)$$

(Ln = Sm, $m = 5$, $n = 6$; Ln = Eu, $m = 7$, $n = 5$)

It is noted that the isolation of both compounds depends on exploring the conditions of hydrothermal reactions. However, it is difficult to optimize the hydrothermal reaction parameters on account of the reaction systems being close. Considering that many factors, such as starting materials, stoichiometry, pH value, filling volume and temperature, may affect the construction of the final products, we carried out a number of parallel experiments to understand the effect from above-mentioned factors. The parallel experiments were carried out by varying the reaction temperature from 80 to 160 °C, and synchronously keeping the concentration of the reactants, pH value, time, and filling volume unchangeable. A series of 3D compounds were obtained at 160 °C just as in our previous work [18], and with the temperature decreased, 2D compound for **1** was obtained at 130 °C and 1D compound for **2** was formed below 110 °C. Taking the realities into account, it can be reasoned that reaction temperature has an important influence on the structures of the products and high temperature helps to increase the dimensionality of the products. We also attempted to synthesize compounds **1** and **2** through traditional aqueous reaction by refluxing the same reaction starting materials at 80 °C for 5 h. However, we obtained no crystals but some precipitation after a week, which demonstrates that hydrothermal condition is the requisite for preparing compounds **1** and **2**.

3.2. Structures

The structures of $\{[Sm(H_2O)_5]_2(TeMo_6O_{24})\} \cdot 6H_2O$ (**1**) and $\{[Eu(H_2O)_7]_2(TeMo_6O_{24})\} \cdot 5H_2O$ (**2**) are both made of typical Anderson-type polyoxoanion $[TeMo_6O_{24}]^{6-}$. The building block $[TeMo_6O_{24}]^{6-}$ belongs to the A-type Anderson structure with a D_{3d} symmetry, which consists of seven edge-sharing octahedron, six of which are $\{MoO_6\}$ octahedron, arranged hexagonally around the central $\{TeO_6\}$ octahedron. The six molybdenum atoms form a regular hexagon. The Te(VI) atom is surrounded octahedrally by six oxygen atoms. The Te–O bond lengths and the O–Te–O bond angles summarized in Table S1 and S2 show only slight distortion of the TeO_6 octahedron. Mo–O distances as expected are divided into three groups: Mo–O_t, 1.69–1.74 Å; Mo–O_b, 1.90–1.96 Å; and Mo–O_c, 2.23–2.29 Å, which are similar to those reported in other compounds containing the $[TeMo_6O_{24}]^{6-}$ anion [20].

Single-crystal X-ray diffraction study reveals that the asymmetric unit of **1** contains half a formula unit, namely, half of a polyoxoanion $[TeMo_6O_{24}]^{6-}$, a $[Sm(H_2O)_5]^{3+}$ cation, and 3 lattice waters, as shown in Fig. 1. Further studies reveal that the structure of **1** is a 2D layer constructed from Anderson-type anions $[TeMo_6O_{24}]^{6-}$ and bridging $\{Sm(H_2O)_5\}$ groups. Each polyoxoanion $[TeMo_6O_{24}]^{6-}$ provides eight terminal oxygen atoms for the coordination of six Sm atoms in a center. Three Sm atoms stand on one side of the planar structure of the Anderson polyoxoanion, and the other three on the opposite side of the planar structure, which results in the six Sm atoms relating to each other by central symmetry. Each Sm atom is nine-coordinate bonding to five oxygen atoms from water molecules and four terminal oxygen atoms of three Anderson-type anions, leading to a distorted tricapped-trigonal prism coordination geometry. The connection of alternate $[TeMo_6O_{24}]^{6-}$ and Sm^{3+} cations forms a unique 2D framework, parallel to the *ab* plane (Fig. 2), which represents the first example of 2D layer compounds constructed from $[TeMo_6O_{24}]^{6-}$ with rare-earth ions.

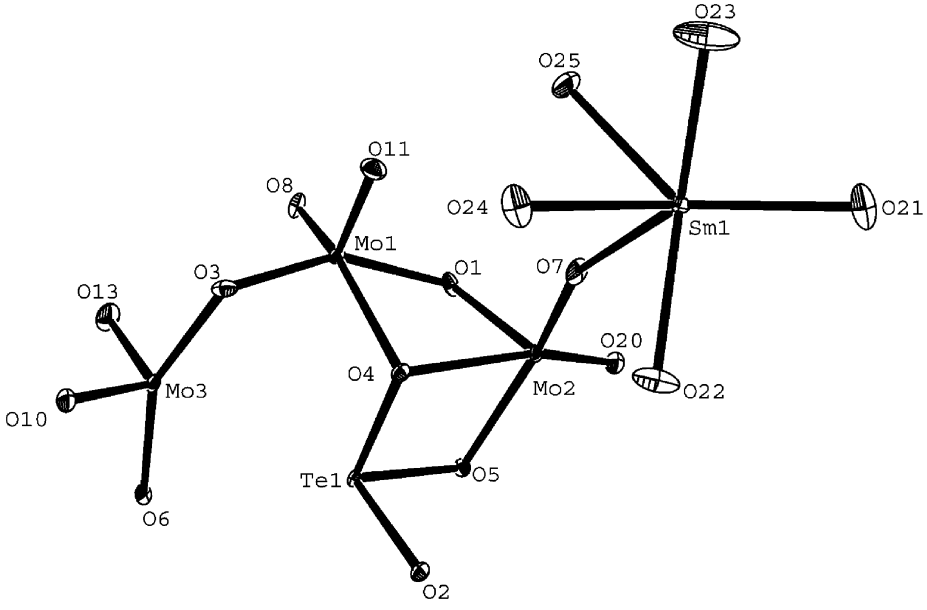

Fig. 1

Compound **2** is assembled by $[TeMo_6O_{24}]^{6-}$ polyoxoanion, $[Eu(H_2O)_7]^{3+}$, and lattice water molecules. The asymmetric unit of **2** is composed of half of a polyoxoanion, a $[Eu(H_2O)_7]^{3+}$, and 2.5 lattice water molecules (Fig. 3). The structure is formed by Anderson-type anions $[TeMo_6O_{24}]^{6-}$ linked by Eu^{3+} ions to yield a polymer chain running along the *c*-axis (Fig. 4). The Anderson anion acts as a tetradentate ligand coordinating four Eu atoms through the terminal oxygen atoms. Each Eu atom has a coordination number of nine and is in a distorted tricapped-trigonal prism environment formed by the two terminal oxygen atoms from two $[TeMo_6O_{24}]^{6-}$ anions and seven oxygen atoms from water molecules, and the Eu atom occupies sites with low symmetry and without an inversion center (Fig. 5).

This structure is similar with those reported before [11,12,14]; however, the connectivity behavior between Anderson anions and rare-earth ions is not completely same, although these compounds exhibit 1D chain-like structure. Anderson anions usually act as multidentate ligands for rare-earth ions (4 for Ce, Pr, Nd, Eu, and Gd; 3 for Tb, Dy, Ho, and Er; 6 for La) and the coordination sphere of the Ln^{III} atoms also has difference, that is, their coordination numbers are 9 (for La, Ce, Pr, Nd, Eu, and Gd) and 8 (for Tb, Dy, Ho, and Er), respectively. Thus, so-formed 1D chains are not fully identical. Thereinto, **2** is isomorphic with those reported compounds of Ce, Pr, and Nd. Compared with the Eu-containing compounds reported previously, it was found that their components and structures were distinct though the so-formed 1D chain was similar. In the reported structure [12], there existed two crystallographically independent $[TeMo_6O_{24}]^{6-}$ anions. One of the ions acted as a tetradentate ligand for the rare-earth ions, the second one was surrounded by potassium ions and crystal water and had no bonding to the rare-earth ions. In our compound, there is only one 1D chain-like structure, which is formed by $[TeMo_6O_{24}]^{6-}$ linked by Eu^{3+} ions.

The bond valence sum calculations [21] indicate that the range and average valence sum for the Mo atoms are 5.92–6.04 and 5.98 for 1, 5.99–6.03 and 6.01 for **2**, respectively. The valence sums for

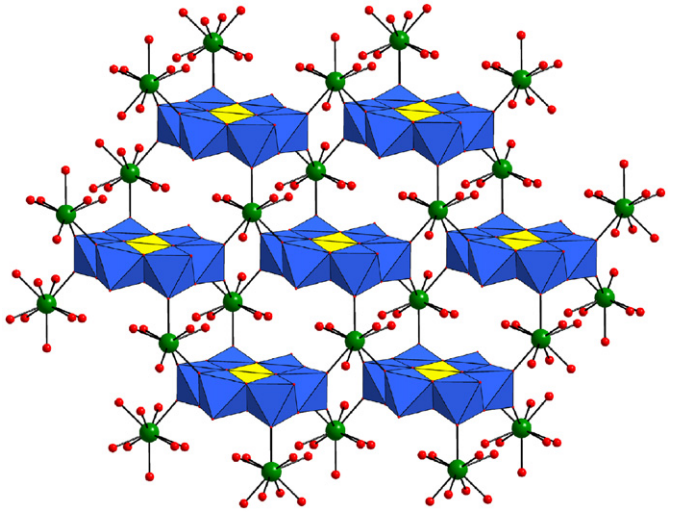

Fig. 2

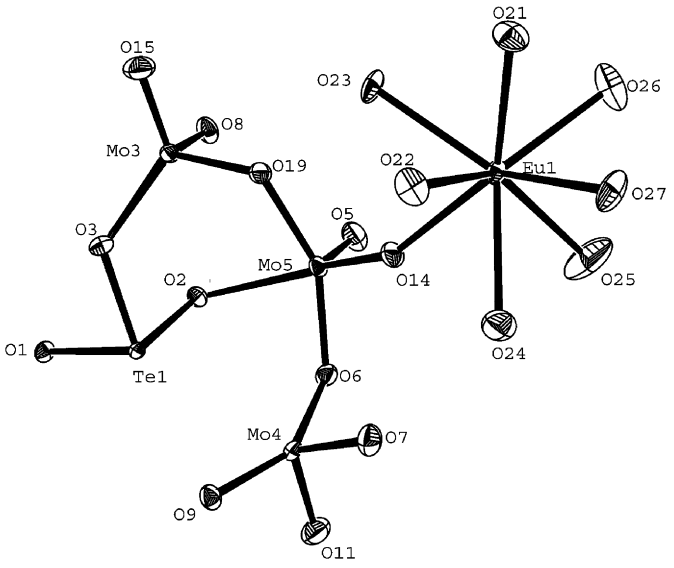

Fig. 3

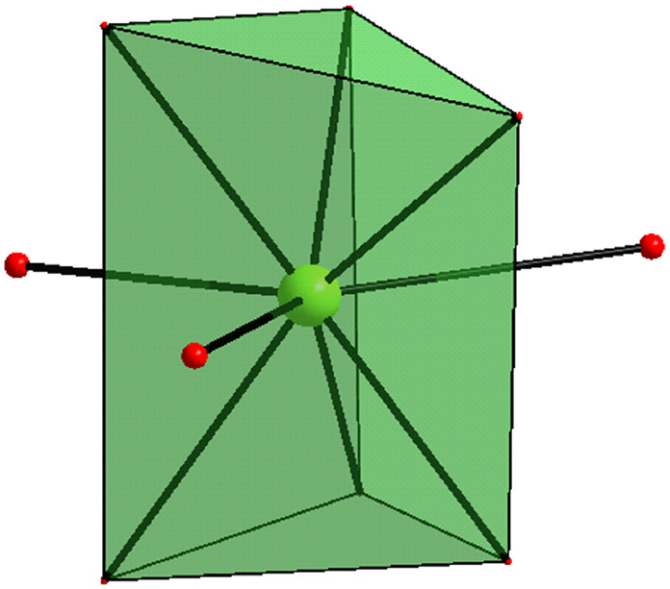

Fig. 5

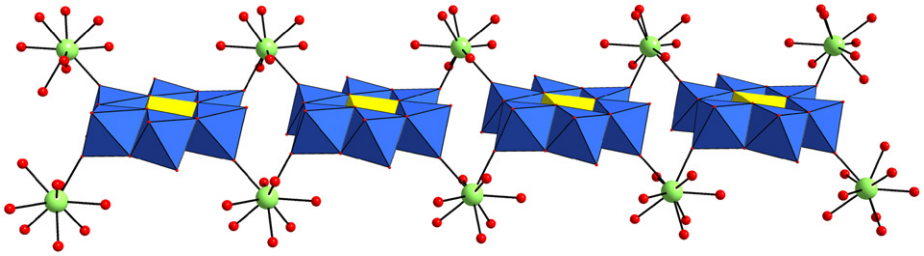

Fig. 4

Sm and Eu atoms are 3.29 and 3.16, and sums for Te atoms are 5.88 in **1** and 5.77 in **2**, respectively. All these values/average values are approximately in accordance with the expected bond valence: Mo, 6.00; Sm, 3.00; Eu, 3.00; Te, 6.00 according to their compositions.

3.3. IR spectroscopy

The IR spectra of both compounds exhibit similar features (Fig. S1). The low-wavenumber characteristic peaks are attributed to the Anderson anion $[TeMo_6O_{24}]^{6-}$ [22]. The characteristic bands between 1000 and 850 cm^{-1} are assigned to the Mo–O_t stretching vibration, the bands between 750 and 530 cm^{-1} are assigned to the Mo–O_b stretching vibration, and the absorption peaks below 450 cm^{-1} are regarded as Mo–O_c stretching vibration. A broad feature at about 3400 cm^{-1} in the IR spectra of both compounds must be assigned to the absorptions of coordinated and lattice water molecules.

3.4. Thermogravimetric analyses

The thermogravimetric analyses (TGA) were performed with the N_2 atmosphere for both compounds in the range 20– 600 °C. The TGA curve of compound **1** exhibits two continuous weight loss stages below 490 °C (Fig. S2), corresponding to the release of all lattice water molecules and coordination water molecules. The total weight loss of 17.35% agrees with the calculated value of 17.28%. The TGA curve of compound **2** exhibits similar weight loss stages to those of compound **1** (Fig. S3). The whole weight loss of 19.81% is in agreement with the calculated value of 19.90%.

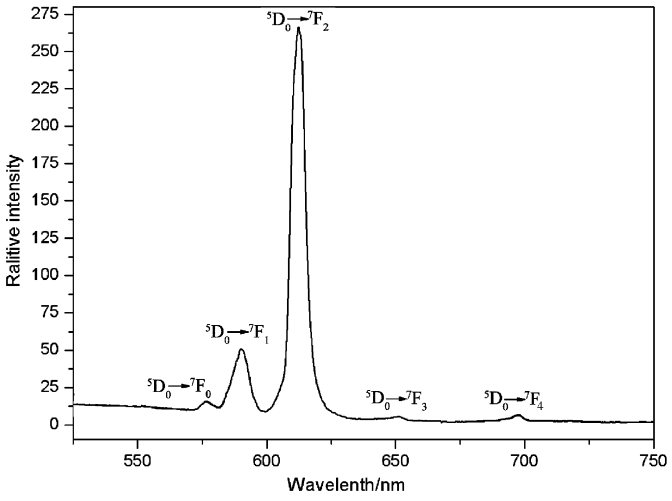

Fig. 6

3.5. Luminescence property

We have measured the photoluminescence spectrum of powder samples of compound **2** at room temperature, which exhibits the characteristic transition of the Eu^{3+} ion under the excitation wavelengths (395 nm), as shown in Fig. 6. The emission bands at 577, 591, 613, 650, and 695 nm correspond to the $^5D_0 \rightarrow ^7F_0$, $^5D_0 \rightarrow ^7F_1$, $^5D_0 \rightarrow ^7F_2$, $^5D_0 \rightarrow ^7F_3$, and $^5D_0 \rightarrow ^7F_4$ transitions, respectively. The $^5D_0 \rightarrow ^7F_0$ transition is strictly forbidden by symmetry. As the $^5D_0 \rightarrow ^7F_0$ transition is observed, the spectrum reveals that Eu^{3+} in **2** occupies sites with low symmetry and without an inversion center, which is consistent with the crystal structures. The $^5D_0 \rightarrow ^7F_1$ and $^5D_0 \rightarrow ^7F_2$ transitions, magnetic and electric dipole transitions, respectively, are clearly observed in the photoluminescence spectrum of **2**. The intensity of the $^5D_0 \rightarrow ^7F_1$ transition depends only slightly on the nature of the environment of the Eu^{3+} center; however, the intensity of the $^5D_0 \rightarrow ^7F_2$ transition is extremely sensitive to chemical bonds in the vicinity of Eu^{3+}, which increases as the site symmetry of the Eu^{3+} center decreases, so the $I(^5D_0 \rightarrow ^7F_2)/I(^5D_0 \rightarrow ^7F_1)$ ratio is widely used as a measure of the coordination state and site symmetry of the rare earth [23–25]. For **2**, the intensity ratio $I(^5D_0 \rightarrow ^7F_2)/I(^5D_0 \rightarrow ^7F_1)$ is equal to ca. 4.6, which also indicates the low site symmetry of the Eu^{3+} ion, and the intense $^5D_0 \rightarrow ^7F_2$ transition points to a highly polarizable chemical environment around the Eu^{3+} ion that is responsible for the brilliant red emission of the compound. It is noteworthy that the red luminescence from the colorless and transparent crystals under UV irradiation (365 nm) is so intense that it can be observed macroscopically (Fig. 7).

4. Conclusions

In summary, two compounds constructed by Anderson polyoxoanion building blocks and rare-earth ions have been isolated under hydrothermal conditions; furthermore, the temperature has an important influence on the structures of the compounds in our experiments. Meanwhile, the stability of $[TeMo_6O_{24}]^{6-}$ polyoxoanion in the hydrothermal conditions provides a feasibility for the further construction of novel Anderson-type polyoxometalates by hydrothermal reactions. Some luminescent information on rare-earth-contained Anderson-type compound is given, and the compound with intense luminescence may serve as advanced materials, efficiently, for red light emitting devices.

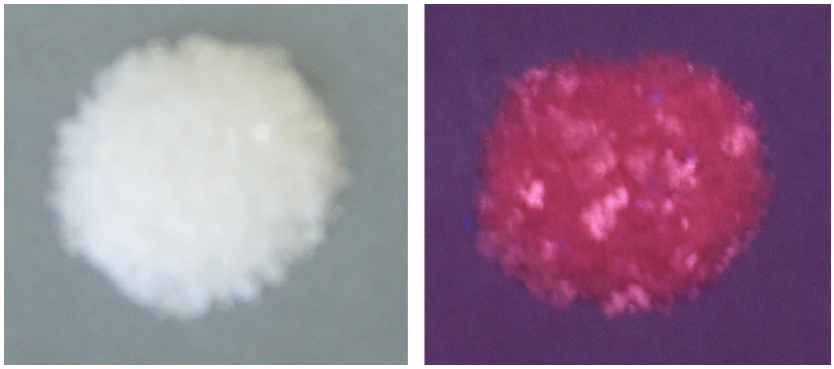

Fig. 7

Acknowledgments

This work was supported by the National Science Foundation of China (Grant no. 20571014), the Program for New Century Excellent Talents in University (NCET-07-0169), and the Analysis and Testing Foundation of Northeast Normal University.

Appendix A. Supplementary material

Supplementary material associated with this article can be found in the online version at doi:10.1016/j.jssc.2008.05.023.

References

[1] M.T. Pope, A. Müller, Angew. Chem., Int. Ed. Engl. 30 (1991) 34–48.
[2] M.T. Pope, Heteropoly and Isopoly Oxometalates, Springer, New York, 1983.
[3] C.L. Hill (Ed.), Chem. Rev. 98 (1998) 1–2.
[4] M.T. Pope, A. Müller (Eds.), Polyoxometalate Chemistry from Topology via Self-Assembly to Applications, Kluwer Academic Publishers, The Netherlands, 2001.
[5] C.L. Hill, C.M. Prosser-McCartha, Coord. Chem. Rev. 143 (1995) 407–455.
[6] S.X. Liu, D.H. Li, L.H. Xie, H.Y. Cheng, X.Y. Zhao, Z.M. Su, Inorg. Chem. 46 (2006) 8036–8040.
[7] M. Sadakane, M.H. Dickman, M.T. Pope, Angew. Chem., Int. Ed. Engl. 39 (2000) 2914–2916.
[8] J.F. Cao, S.X. Liu, R.G. Cao, L.H. Xie, Y.H. Ren, C.Y. Gao, L. Xu, J. Chem. Soc. Dalton Trans. (2008) 115–120.
[9] X.T. Zhang, D.q. Wang, J.M. Dou, S.S. Yan, X.X. Yao, J.Z. Jiang, Inorg. Chem. 45 (2006) 10629–10635.
[10] V. Shivaiah, P.V.N. Reddy, L. Cronin, L. Cronin, S.K. Das, J. Chem. Soc. Dalton Trans. (2002) 3781–3782.
[11] D. Drewes, E.M. Limanski, B. Krebs, Eur. J. Inorg. Chem. (2004) 4849–4853.
[12] D. Drewes, E.M. Limanski, B. Krebs, J. Chem. Soc. Dalton Trans. (2004) 2087–2091.
[13] D. Drewes, B. Krebs, Z. Anorg. Allg. Chem. 631 (2005) 2591–2594.
[14] A.B. Yusov, I.A. Charushnikova, A.M. Fedoseev, Zh. Nerog. Khim. 49 (2004) 1481–1487.
[15] H.Y. An, Y.G. Li, D.R. Xiao, E.B. Wang, C.Y. Sun, Cryst. Growth Des. 6 (2006) 1107–1112.
[16] H.Y. An, D.R. Xiao, E.B. Wang, Y.G. Li, X.L. Wang, L. Xu, Eur. J. Inorg. Chem. (2005) 854–859.
[17] H.Y. An, D.R. Xiao, E.B. Wang, C.Y. Sun, L. Xu, J. Mol. Struct. 743 (2005) 117–123.
[18] B. Gao, S.X. Liu, L.H. Xie, M. Yu, C.D. Zhang, C.Y. Sun, H.Y. Cheng, J. Solid State Chem. 179 (2006) 1681–1689.
[19] G.M. Sheldrick, SHELXS-97, Program for Crystal Structure Solution, University of Göttingen, Germany, 1997.
[20] A.J. Bridgeman, G. Cavigliasso, J. Phys. Chem. A. 107 (2003) 6613–6621.
[21] I.D. Brown, D. Altermatt, Acta Crystallogr. Sect. B 41 (1985) 244.
[22] I.L. Botto, C.I. Cabello, H.J. Thomas, Mater. Chem. Phys. 47 (1997) 37–45.
[23] R.G. Cao, S.X. Liu, L.H. Xie, Y.B. Pan, J.F. Cao, Y. Liu, Inorg. Chim. Acta. 361 (2008) 2013–2018.
[24] Y. Lu, Y. Xu, Y.G. Li, E.B. Wang, X.X. Xu, Y. Ma, Inorg. Chem. 45 (2006) 2055–2060.
[25] S. Biju, D.B. Ambili Raj, M.L.P. Reddy, B.M. Kariuki, Inorg. Chem. 45 (2006) 10651–10660.